Environmental Microbiology (2016) 00(00), 00–00 doi:10.1111/1462-2920.13483

Meltwater export of prokaryotic cells from the Greenland ice sheet

Karen A. Cameron,[1,2*] Marek Stibal,[1,2,3] Jon R. Hawkings,[4] Andreas B. Mikkelsen,[2] Jon Telling,[4] Tyler J. Kohler,[3] Erkin Gözdereliler,[1,2] Jakub D. Zarsky,[3] Jemma L. Wadham[4] and Carsten S. Jacobsen[2,5]

[1]*Department of Geochemistry, Geological Survey of Denmark and Greenland (GEUS), Copenhagen, Denmark.*

[2]*Center for Permafrost (CENPERM), University of Copenhagen, Copenhagen, Denmark.*

[3]*Department of Ecology, Charles University in Prague, Prague, Czech Republic.*

[4]*Bristol Glaciology Centre, School of Geographical Sciences, University of Bristol, UK.*

[5]*Department of Environmental Science, Aarhus University, Roskilde, Denmark.*

Summary

Microorganisms are flushed from the Greenland Ice Sheet (GrIS) where they may contribute towards the nutrient cycling and community compositions of downstream ecosystems. We investigate meltwater microbial assemblages as they exit the GrIS from a large outlet glacier, and as they enter a downstream river delta during the record melt year of 2012. Prokaryotic abundance, flux and community composition was studied, and factors affecting community structures were statistically considered. The mean concentration of cells exiting the ice sheet was 8.30 $\times$ 10^4 cells mL^{-1} and we estimate that $\sim$1.02 $\times$ 10^{21} cells were transported to the downstream fjord in 2012, equivalent to 30.95 Mg of carbon. Prokaryotic microbial assemblages were dominated by Proteobacteria, Bacteroidetes, and Actinobacteria. Cell concentrations and community compositions were stable throughout the sample period, and were statistically similar at both sample sites. Based on our observations, we argue that the subglacial environment is the primary source of the river-transported microbiota, and that cell export from the GrIS is dependent on discharge. We hypothesise that the release of subglacial microbiota to downstream ecosystems will increase as freshwater flux from the GrIS rises in a warming world.

*For correspondence: E-mail: kac.geus@gmail.com; Tel.: +44 7764 968 773

Introduction

The Greenland Ice Sheet (GrIS) has experienced a significant increase in annual surface melt over the past three decades (Fettweis *et al.*, 2011), with a net ice mass loss over the last two decades (Rignot *et al.*, 2011; Shepherd *et al.*, 2012), largely as the result of rising Arctic air temperatures (Hanna *et al.*, 2008). Meltwater accounts for approximately a third of this mass loss (Bamber *et al.*, 2012), the majority of which gets routed through englacial and subglacial environments by moulins and crevasses (Clason *et al.*, 2015) before emerging from the glacial system (Bartholomew *et al.*, 2011; Chandler *et al.*, 2013). By 2100, the annual freshwater flux from the GrIS is estimated to increase by 200 – 1600 GT y^{-1} in comparison to the 1980 – 1999 mean (equivalent to $\sim$2 – 13 cm sea level rise; Fettweis *et al.*, 2012), highlighting the sensitivity of the world's second largest source of frozen freshwater to a changing climate.

Recent work has demonstrated the importance of glacial meltwaters in delivering nutrients to the polar oceans (Bhatia *et al.*, 2013; Wadham *et al.*, 2013; Hawkings *et al.*, 2014; 2015; Lawson *et al.*, 2014a,b). Projected future increases in meltwater runoff (Fettweis *et al.*, 2012) and hydrologically active drainage areas (Leeson *et al.*, 2014) in a warming climate are anticipated to elevate dissolved and particulate material released from subglacial environments (Hudson *et al.*, 2014; Hawkings *et al.*, 2015). Furthermore, anomalous events, such as atypical increases in supraglacial melt and supraglacial lake drainage (Hasholt *et al.*, 2006; Bartholomew *et al.*, 2011) may increase in frequency, and influence glacial motion and augment subglacial sediment release (Bartholomew *et al.*, 2011; Hudson *et al.*, 2014). The GrIS has recently experienced several extreme melt events (Comiso, 2006; Tedesco, 2007). The summer of 2012 had the most extensive and long lasting melt event, with the greatest

J_ID: EMI Customer A_ID: EMI13483 Cadmus Art: EMI13483 Ed. Ref. No.: 13483 Date: 10-August-16 Stage: Page: 2

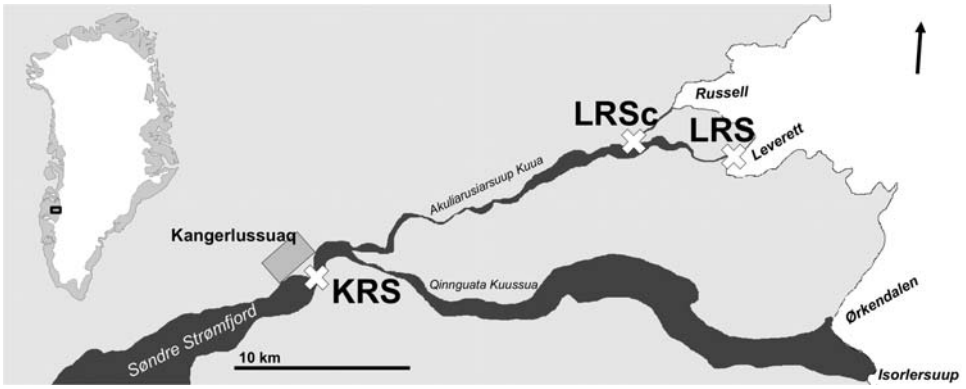

Fig. 1. Schematic of study site locations (white crosses) within the Kangerlussaq locality, and an inset map of Greenland showing the overall location (black rectangle). Glaciated areas are depicted in white and ice-free areas are depicted in light grey. Watson river and the fjord that it feeds is shown in dark grey. Arrow depicts north.

observed runoff and net ice mass loss since satellite recordings began in 1979 (Tedesco *et al.*, 2013).

Subglacial environments contain active microbial communities (Sharp *et al.*, 1999; Skidmore *et al.*, 2000; Yde *et al.*, 2010; Stibal *et al.*, 2012b; Dieser *et al.*, 2014) which mediate chemical weathering (Wadham *et al.*, 2010; 2013; Montross *et al.*, 2013), resulting in the release of solutes and nutrients to subglacial meltwater flows (Tranter *et al.*, 2005; Wadham *et al.*, 2010; 2013; Montross *et al.*, 2013; Hawkings *et al.*, 2015). Bacterial community profiles sampled from waters that emanate from beneath Russell Glacier, an outlet glacier southwest of the GrIS, are distinct from nearby supraglacial waters, indicating that microbial communities specific to subglacial environments are released from beneath the ice sheet (Dieser *et al.*, 2014). While recent studies have reported the microbial abundance of GrIS supraglacial snow and ice samples to range from $\sim 10^2$ to 10^6 cells mL^{-1} (Cameron *et al.*, 2015; Stibal *et al.*, 2015a), and subglacial basal ice samples to have $\sim 9 \times 10^5$ cells g^{-1} (Stibal *et al.*, 2012a), there are currently no estimates for the magnitude of cells exported from glacial environments during the melt season. Microbes transported from glaciers have the potential to influence estuary ecosystems through the import of environmentally suited cells, which may alter nutrient cycles and community composition (Garneau *et al.*, 2006; Gutiérrez *et al.*, 2015). The quantification and description of exported cells is therefore necessary to discern what role they might play in downstream habitats.

Here we characterize and quantify microbial cells within meltwater samples from two sites separated by ~30 km along the Watson River in southwest Greenland over the 2012 melt season (Fig. 1). Water was captured at the first site as it exited the southwest of the GrIS, near the Leverett Glacier outlet. Water was also collected at a second downstream site, fed by four glacier outlets, prior to entering the river delta of the Søndre Strømfjord. To evaluate spatial and temporal patterns in the microbial assemblages, we monitored and compared cell concentrations and community structures at both sites using quantitative PCR (qPCR) and 16S rRNA gene sequencing approaches, and used multivariate analyses to identify factors associated with the presence and diversity of the exported microbes. To reduce qPCR analysis biases associated with gene copy quantification from DNA extracts of sediment-laden waters (Stibal *et al.*, 2015a), qPCR standards were generated using DNA extracts from artificial river water samples spiked with prokaryotic cultures, and using copy number per cell conversion factors that were tailored to the amplicon diversity of each sample. Microbial cell export was quantified by combining cell abundance with parallel hydrological records (discharge and suspended sediment). Lastly, the nutritional significance of these river-transported microbiota is considered using upscaling to estimate the magnitude of microbial release across the entire GrIS.

Results

Discharge rates, sediment loads and chemistry

Mean daily discharge at KRS ranged from ca 80 m^3 s^{-1}, at the start and end of the sample period, to ca 2800 m^3 s^{-1}, with two distinct peaks; one in early-mid July (DOY; 190-198), and one late-July to early-August (DOY; 211-221, Fig. 2a). The mean annual volume of water passing KRS from 2007 to 2013 was $\sim 4.44 \pm 2.28$ km^3. Mean KRS daily sediment load was < 1.5 g L^{-1} before May 29 (DOY; 150) and after September 7 (DOY; 251), and fluctuated between 1.44 g L^{-1} and 4.73 g L^{-1} between these dates (Fig. 2a). DOC values are reported in Supporting Information Table S2.

Cell abundance

Cell abundance, determined by qPCR analysis, was calculated to be between 9.48×10^3 cells mL^{-1} to 7.44×10^5 cells mL^{-1} for all samples (Fig. 2b; mean abundance $1.15 \times 10^5 \pm 1.38 \times 10^5$ cells mL^{-1}). Differences between mean cell abundances calculated from LRS and KRS across the sampling season were not found to be significantly

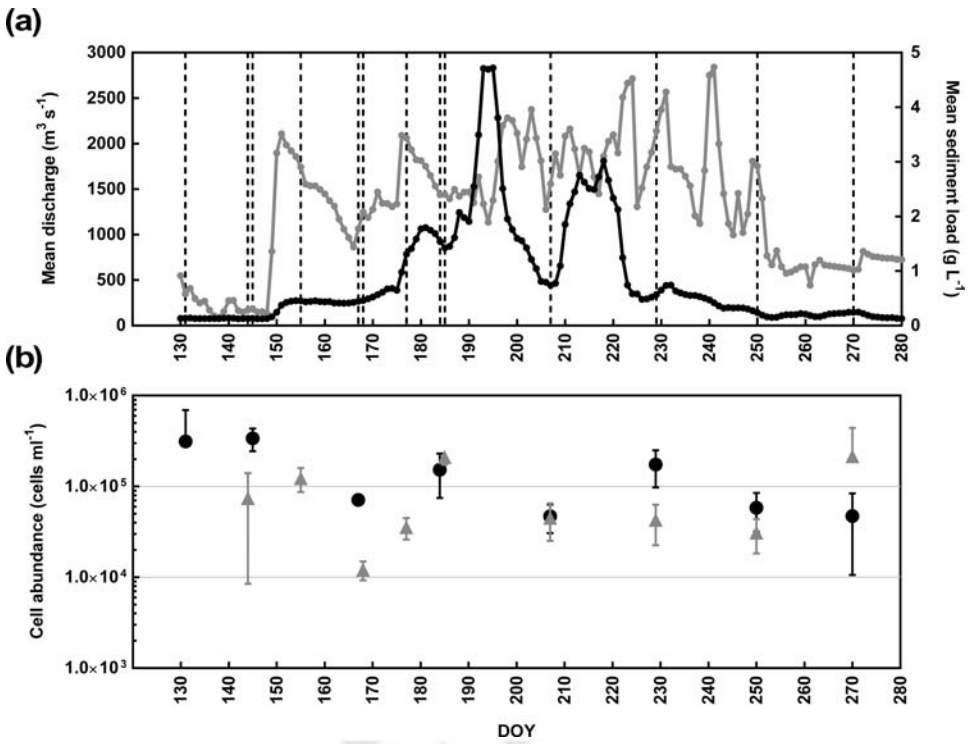

Fig. 2. (a) Discharge rates and sediment loads measured at KRS. Black depicts discharge, grey depicts sediment load. Dashed lines indicate sampling days. (b) qPCR 16S rRNA abundance analyses. Grey triangles depict LRS analyses, black circles depict KRS analyses. Error bars depict standard deviations.

different using a two-tailed *t*-test (LRS mean; 8.30 x $10^4 \pm 9.88$ x 10^4 cells mL^{-1}, KRS mean; 1.50 x $10^5 \pm 1.65$ x 10^5 cells mL^{-1}, $t = 1.30$, $p = 0.21$). When a two-tailed paired *t*-test was performed using mean values from pairwise dates ($n = 7$), no statistically significant difference was found ($t = 0.71$, $p = 0.51$). No significant correlation was found between cell abundance at LRS or KRS when calculated against discharge rates or sediment loads, with all Pearson's coefficient *r* values being $< \pm$ 0.55 and all *p* values being > 0.16., The mean abundance of archaea within LRS and KRS samples was 2.91 x $10^3 \pm 2.19$ 10^3 cells mL^{-1} and 2.65 x $10^3 \pm 2.52$ x 10^2 cells mL^{-1}, respectively, based on qPCR analysis using archaea specific primers. No correlation was found between the abundance of archaea and discharge rates when a Pearson's correlation analysis was performed ($r = -0.21$, $p = 0.14$).

Amplicon sequencing read output

After sequence processing, the total number of reads generated from all samples was 889,724, with an average of $17{,}795 \pm 4678$ reads per sample. Sequences were rarefied to 8670 sequences per sample, which resulted in the omission of a LRS June 3 replicate. After rarefaction the mean number of OTU clusters per sample was 621.59 ± 225.29. The difference between the mean CatchAll calculated alpha diversity of the rarefied datasets was not significant when calculated using a two-tailed Mann-Whitney U test (mean LRS CatchAll calculated alpha diversity; 990.99 ± 331.04, mean KRS CatchAll calculated alpha diversity; 1404.53 ± 668.70, *Z-score* $= -1.91$, $p = 0.06$).

Community composition

KRS and LRS rarefied communities consisted of OTU that were most closely related to sequences belonging to 47 different phylum-level classifications. The majority of amplicons were most closely related to six phylum level classifications; Proteobacteria ($65.33 \pm 4.85\%$; 6.95 x $10^4 \pm 8.44$ x 10^4 cells mL^{-1}), Bacteroidetes ($20.66 \pm 4.36\%$; 3.53 x $10^4 \pm 3.88$ x 10^4 cells mL^{-1}), Actinobacteria ($6.49 \pm 2.22\%$; 5.44 x $10^3 \pm 9.08$ x 10^3 cells mL^{-1}), Verrucomicrobia ($1.75 \pm 1.11\%$; 1.06 x $10^3 \pm 1.42$ x 10^3 cells mL^{-1}), Chloroflexi ($1.16 \pm 0.69\%$; 9.34 x $10^2 \pm 1.36$ x 10^3 cells mL^{-1}) and Acidobacteria ($1.08 \pm 0.58\%$; 6.65 x $10^2 \pm 9.74$ x 10^2 cells mL^{-1}; Fig. 3a and b). The remaining 41 phylum-level classifications each had a mean amplicon relative abundance of $< 1\%$. At the order level, the most dominant OTU were most closely related to Burkholderiales ($32.76 \pm 9.31\%$; 2.90 x $10^4 \pm 3.44$ x 10^4 cells mL^{-1}), Flavobacteriales ($13.41 \pm 6.78\%$; 2.47 x $10^4 \pm 2.90$ x 10^4 cells mL^{-1}) and Methylophilales ($12.90 \pm 4.74\%$; 1.98 x $10^4 \pm 2.22$ x 10^4 cells mL^{-1}; Fig. 3c and d), and OTU relating to a further 234 order level classifications were identified. Cyanobacteria related sequences, a potential proxy for supraglacial water inputs, comprised $0.16 \pm 0.12\%$ (2.04 x $10^2 \pm 3.76$ x 10^2 cells mL^{-1}) in each community, and no relationship was

J_ID: **EMI** Customer A_ID: **EMI13483** Cadmus Art: **EMI13483** Ed. Ref. No.: **13483** Date: **10-August-16** Stage: Page: **4**

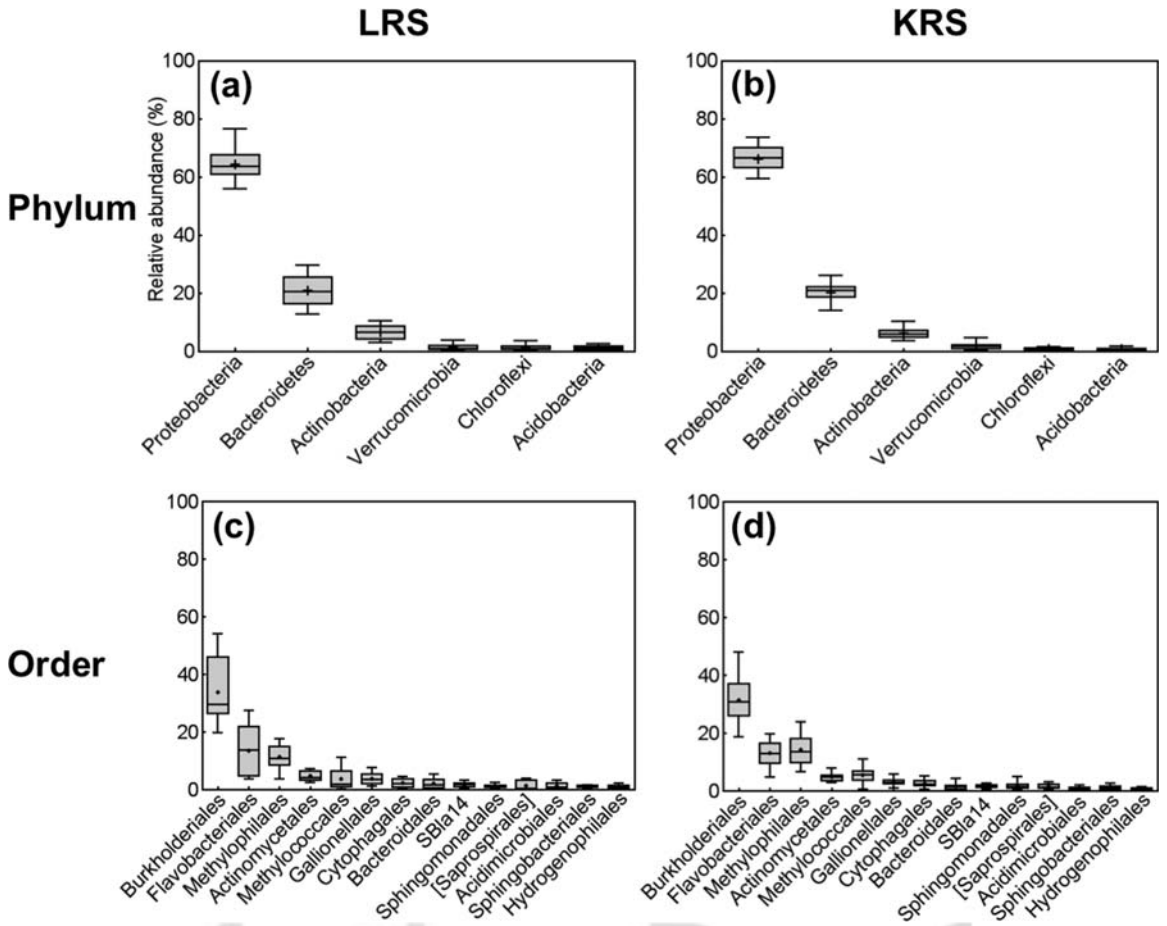

Fig. 3. Box plot with whiskers showing the relative abundance range, median and mean for OTU grouped by phylum-; (a), (b) and order-; (c), (d) level classifications, and by LRS; (a), (c) and KRS; (b), (d) sample sites throughout the sampling period. Grey boxes depict 25th - 75th percentiles, whiskers depict maximum and minimum values, box lines depict median values, and cross depicts mean values. Only classifications with $\geq$1% mean relative abundance are shown. Order names in square brackets are suggested annotations from the Greengenes database.

found between discharge and their abundance when a Pearson's correlation analysis was performed ($r = -0.22$, $p = 0.12$). The domain Archaea constituted $0.18 \pm 0.10\%$ and $0.23 \pm 0.14\%$ of the total LRS and KRS prokaryotic amplicon communities. Archaea related amplicons were predominantly most closely related to Euryarchaeota ($0.06 \pm 0.05\%$) and Crenarchaeota ($0.05 \pm 0.04\%$).

Factors contributing to community variability. Two-way crossed ANOSIM analysis of amplicon communities grouped by location and by closest sampling date found them to be highly similar (location grouped *GlobalR* = 0.934, $p = 0.001$, date grouped *GlobalR*; 0.997 $p = 0.001$). Principal component analysis (PCA) identified that 65% of variance in microbial community structure was explained within the first 4 axes. To identify the most significant factors influencing microbial community structure, a redundancy analysis (RDA) was performed with discharge, DOY, location (LRS vs. KRS) and mean daily sediment load as the explanatory variables. These variables were found to account for 40.2% of variance, with discharge accounting for the largest contribution (22.3% of variance explained, *pseudoF* = 13.5, $p = 0.0025$), followed by DOY (10.7%, *pseudoF* = 7.3, $p = 0.0025$) and location (4.8%, *pseudoF* = 3.4, $p = 0.0063$).

Mean daily sediment load was found to be insignificant in this analysis ($p = 0.068$). A subset of data from LRS was also analysed from when water chemistry data were available (DOY 144-207; see Supporting Information Table S2, S3 and S4). PCA explained 74.2% of total variance in the data within the first 4 axes. When constrained by DOY, discharge, mean daily sediment load and water chemistry, redundancy analysis explained 73.4% of variance within the first 4 axes. Interactive forward selection identified the most significant factors, including discharge, pH and nitrate concentration (each of them individually explaining 33% of variance at $p = 0.002$), to be highly collinear. Mean daily sediment load and DOY were also found significant in the

ID: **prabhakaran.m** Time: 21:17 I Path: //10.18.11.53/Home$/prabhakaran.m$/JW-EMI#160358

analyses ($p < 0.001$), however, the robustness of this analysis should be taken with caution due to the low number of samples and high number of predictors.

One-way ANOSIM analysis of communities from LRS and the secondary site, LRSc, found them to be highly similar (*GlobalR* = 0.987, $p = 0.001$).

Discussion

The abundance of cells within meltwater exiting Leverett Glacier and sampled at the LRS site was stable throughout the study period, indicating that GrIS biomass release scales with meltwater discharge. From this, it follows that fluxes of GrIS-derived biomass will increase alongside climate-influenced elevated melt rates in the future (Mernild *et al*., 2010; Fettweis *et al*., 2012), similar to dissolved and particulate material release (Hudson *et al*., 2014; Hawkings *et al*., 2015). Community composition at the OTU level and mean cell concentrations calculated downstream at KRS were found to be statistically similar to those at LRS, despite almost 30 km of river length between sites and the inclusion of water from both of the Watson River tributaries at the KRS site. This result suggests that terrestrial microbial inputs were minimal, and that the neighbouring Ørkendalen and Isorlersuup glaciers to the south of Leverett Glacier are releasing similar microbial assemblages in similar discharge-influenced cell concentrations. This study therefore indicates that the glacial environment is the predominant source of biomass transported downstream to the Søndre Strømfjord delta, and in this respect, we can view the Watson River drainage system as a conceptual "pipe" connecting the glacial environment, and its associated microbes, to the estuary. This model contrasts to previous studies that have found downstream river communities to be seeded by adjacent soils (Crump *et al*., 2012), modified by flowing through lentic environments (Crump *et al*., 2007; Adams *et al*., 2014), and varying with catchment area (Savio *et al*., 2015). In the case of the sampled Watson River, voluminous glacial melt may markedly dilute smaller riparian and lake signal inputs, and bedrock substrata may limit hyporheic exchange. Furthermore, we estimate that the river transit time between LRS and KRS sample points was $2.7 - 8.1$ h, using estimates of Watson River flow rates ($1 - 3$ m s^{-1}), which is substantially shorted than the multi-day residence time of water traveling through lentic environments (Crump *et al*., 2007; Adams *et al*., 2014); equating to a reduced microbial water residence time during which prokaryotic community compositions can develop, independent of input sources (Adams *et al*., 2014).

Data pertaining to cell concentrations in GrIS glacial meltwaters are currently unreported, however, prokaryotic cells were found to be an order of magnitude more concentrated within LRS samples than within surface ice meltwater samples analysed from Russell Glacier in 2012 (8.38 x $10^3 \pm 9.85$ x 10^3 cells mL^{-1} calculated from 13 samples collected between 7 June and 25 August; Cameron and Junge; unpublished). When compared to surface ice meltwaters from Midre Lovénbreen glacier in Svalbard, waters at LRS were found to be four fold more concentrated than combined bacterial, archaeal and eukaryotic cell concentrations reported by Irvine-Fynn *et al.* (2012; ~2 x 10^4 cells mL^{-1}), and two to four fold higher than concentrations reported by Mindl *et al.* (2007; 1.38 x 10^4 to 4.84 x 10^4 cells mL^{-1}). Prokaryotic cells sampled from LRS and KRS were an order of magnitude less abundant than the bacterioplankton sampled from river and estuary waters of the Lena River, the second largest Arctic Ocean river input (>1.5 x 10^6 cells mL^{-1}; Sorokin and Sorokin, 1996; Dittmar and Kattner, 2003), and were of similar abundance to waters sampled from Mackenzie River, the fourth largest Arctic Ocean river input (6.3 x 10^5 cells mL^{-1}; Garneau *et al*., 2006; Dittmar and Kattner, 2003), and a Patagonian glacial-fed fjord (~10^5 cells mL^{-1}; Gutiérrez *et al*., 2015). Given the size of the Lena and Mackenzie river catchment areas (2.4 x 10^6 km^2 and 1.8 x 10^6 km^2 respectively; Holmes *et al*., 2000; Emmerton *et al*., 2008), the variety of landscapes through which they flow, and the rich marine and terrestrial biotic and nutritional inputs that Patagonian fjord waters receive, the comparable cell abundance of these systems to LRS and KRS waters highlights the notable concentrations of biota that are exported from the GrIS during the melt season. Our study was coincidentally performed during the highest discharge year since records began in 1979 (Tedesco *et al*., 2013), however, most of this melt event was captured during two distinct peaks, which were not sampled in this study (Fig. 2a), and we therefore believe our reported concentrations to be representative estimates. We however note that beyond the filtration of samples through 0.22 μm polyethersulfone filters (Liang and Keeley, 2013), no steps were taken to further reduce or quantify the amplification of extracellular DNA (e.g Nielsen *et al*., 2007, Kim *et al*., 2016), therefore our values may overestimate abundance.

LRS and KRS communities were diverse and dominated by Proteobacteria, Bacteroidetes and Actinobacteria. Like the subglacial outflow waters of Russell Glacier (Dieser *et al*., 2014), samples from both sites were found to have high percentages of OTU that were most closely related to Burkholderiales, and OTU related to Actinomycetales, Flavobacteriales, Methylococcales and Methylophilales were all found to have relative abundances of >1% in both studies. Likewise, OTU related to orders Burkholderiales and Gallionellales, which contain a high numbers of iron-oxidizing chemolithotrophic bacteria, were found to be predominant within these samples (Fig. 3) and within samples taken from the subglacial environment of Robertson Glacier, Canada (Hamilton *et al*., 2013).

Cyanobacteria comprised ~0.2% of samples from both sites, similar to previous reports of subglacial

environments (Hamilton *et al.*, 2013; Dieser *et al.*, 2014). Since Cyanobacteria typically dominate surface ice and associated debris (with up to ~80% relative abundance, Stibal *et al.*, 2015b; Cameron *et al.*, 2016), this result suggests that the majority of biomass within this study originated from the subglacial environment. In contrast, a study from a small subglacial outflow of Russell Glacier found that only 21% of sequences were unique to its subglacial environment (Dieser *et al.*, 2014), while 76% were common to both supra- and subglacial libraries. While the subglacial drainage network of Leverett Glacier is likely substantially more extensive than that of Russell Glacier, leading to a greater subglacial signal in meltwater, caution should nevertheless be taken when using biotic signatures to determine the origins of microbial material.

Of the minimal dissimilarities found between the temporally sampled microbial assemblages, discharge explained between 20-30% of variance, with sample date also being significant. This is likely to be the result of a seasonally-developing subglacial drainage system (Bartholomew *et al.*, 2011; Chandler *et al.*, 2013), facilitating the release of different reserves of subglacial microbiota as the area of subglacial drainage expands further from the margin. Changes in the proportion of supraglacial to subglacial source water may also contribute to the variance in the community structure data; however, the lack of correlation between discharge and the relative abundance of Cyanobacteria does not corroborate this explanation. One way that supra- and subglacial contributions could be discerned is by sampling during "outburst events", which are discreet periods of subglacial flushing that occur several times per melt season (Hawkings *et al.*, 2014). As our sampling regime was not explicitly designed to test this, outburst peaks were not captured in this study (although sample DOY 177 may be on the rising limb of the first outburst, Fig. 2a). Sampling outburst events may offer future insight into the composition and ecology of subglacial microbial communities, and may shed additional light onto potential estuarine contributions.

Over the course of the 2012 melt season, we estimate that a total volume of ~6.83 km^3 of water passed the KRS sample site. The mean cell abundance at KRS was calculated to be 1.50 x 10^5 cells mL^{-1}, which equates to ~1.02 x 10^{21} cells, or ~30.95 Mg of cell associated carbon, ~5.94 Mg of cell associated nitrogen, and ~1.54 Mg of cell associated phosphorus flowing into the fjord (based on mean cellular carbon and nitrogen contents of surface coastal bacterial assemblages; 30.2 fg C $cell^{-1}$ and 5.8 fg N $cell^{-1}$, respectively; Fukuda *et al.*, 1998, and a P:C ratio of 0.05; Fagerbakke *et al.*, 1996, Table 1). Based on mean early- to mid-melt season DOC (0.26 μg mL^{-1}), and mean 2009 and 2010 particulate organic carbon concentrations from Leverett Glacier (2.33 μg mL^{-1}; Lawson *et al.*, 2014b), we estimate that a total of ~17.68 x 10^3 Mg of organic carbon flowed into the fjord during the 2012 melt season, and that cell biomass contributed towards ~0.18% of this (Table 1). Estimates of total organic nitrogen flux to the fjord were calculated to be 1.02 x 10^3 Mg, using mean dissolved organic nitrogen concentrations (0.026 μg mL^{-1}; Wadham *et al.*, submitted) and estimates of particulate nitrogen from Leverett Glacier outflow water sampled in 2015 (0.12 μg mL^{-1}; Kohler, Zarsky, Stibal *et al.*, unpublished). We estimate that cells account for ~1.40% of the total organic nitrogen that flowed to the fjord. Mean total organic phosphorus concentrations were calculated to be 0.03 μg mL^{-1} (dissolved organic phosphorus; DOP; 0.001 μg mL^{-1}; Hawkings *et al.*, 2016, particulate organic phosphorus; 0.03 μg mL^{-1}), amassing to ~ 225.49 Mg of organic P flowing into the fjord, of which we estimate that 0.68% originates from biomass (Table 1). Estimates of the percentage contribution of cells to organic C and N fluxes at KRS were approximately half of those calculated from the four largest Arctic Ocean river inputs (Yenisey, Lena, Ob and Mackenzie rivers, termed "Big-4 Arctic rivers" herein; Table 1). Estimated KRS cellular contributions to DOP was three fold higher than the Big-4 Arctic rivers calculated cellular percentage contribution, however it should be noted that there was an order of magnitude difference between DOP concentrations calculated from Lena River (Dittmar and Kattner, 2003) and Mackenzie River (Emmerton *et al.*, 2008) sampled waters. As far as the authors are aware, the particulate organic phosphorus fraction of the Lena and Mackenzie River systems is unreported so cellular contribution to TOP cannot be commented on.

The mean freshwater runoff across the whole of the GrIS was estimated to be 419.34 ± 54.22 km^3 yr^{-1} between 2000 and 2006 (Fettweis, 2007). Assuming that glacial discharge cell concentrations are homogenous across the GrIS, and that they are stable between melt years, based on cell abundance at KRS we calculate that ~6.29 x 10^{22} cells yr^{-1} are transported from the ice sheet to surrounding environments, equating to ~1900 Mg yr^{-1} of cell associated carbon, ~365 Mg yr^{-1} of cell associated nitrogen, and ~95 Mg yr^{-1} of cell associated phosphorus. This cell flux was at least seventeen times lower than the combined estimated flux from the Big-4 Arctic rivers, which individually have similar annual discharge rates to the estimated annual GrIS freshwater runoff (discharge rates range from 249 - 333 km^3 yr^{-1}, Mackenzie River, to 562 - 577 km^3 yr^{-1}, Yenisey River; Dittmar and Kattner, 2003). The estimated C, N and P nutrient contributions to downstream environments is an order of magnitude lower than exports from the Big-4 Arctic rivers (Table 1). However, while cells within Arctic glacier and ice sheet-fed rivers systems are found to contribute minimally towards nutrient budgets, we argue that the focus of their importance lies within the ability of viable and environmentally suited microorganisms, regardless of their abundance (Wilhelm *et al.*, 2014), to recycle organic nutrients within

J_ID: EMI Customer A_ID: EMI13483 Cadmus Art: EMI13483 Ed. Ref. No.: 13483 Date: 10-August-16 Stage: Page: 7

Table 1. Analyses of the estimated yearly prokaryotic contribution of C, N and P from LRS, KRS, the GrIS and the Big-4 Arctic rivers (Yenisey, Lena, Ob, and Mackenzie rivers).

	LRS; 2012	KRS; 2012 [a]	GrIS; 2000 – 2006 [a,b]	Big-4 Arctic rivers [c]
Discharge (km^3 yr^{-1})	2.2 [d]	6.83 [e]	419.34 [f]	1740 – 1860 [g]
TOC (Mg yr^{-1})	5695.51 [h]	17681.98	1.09 x 10^6	1.40 x 10^7 – 1.75 x 10^7 [g]
TON (Mg yr^{-1})	329.46 [i]	1022.83	62798.18	5.20 x 10^5 – 7.40 x 10^5 [g]
TOP (Mg yr^{-1})	72.63 [j]	225.49	13844.09	–
DOP (Mg yr^{-1})	2.32 [j]	7.19	441.56	23200 – 38000 [k]
Cells yr^{-1} (x10^{20})	1.83	10.25	629.01	>11000 [l]
Estimated cellular C (Mg yr^{-1})	5.52	30.95	1900.30	>33200
% contribution of cellular C	0.10	0.18	–	0.24
Estimated cellular N (Mg yr^{-1})	1.06	5.94	364.94	>6380
% contribution of cellular N	0.78	1.40	–	1.23
Estimated cellular P (Mg yr^{-1})	0.28	1.54	95.01	>1660
% contribution of cellular P	0.38 [m]	0.68 [m]	–	>7.15 [n]
	12.09 [n]	21.41 [n]		

Percentage contibution of cellular nutrient refers to the calculated percentage of estimated annual mass flux of cell associated nutrient relative to total annual mass flux of the nutrient.
a. Chemistry based on analyses from LRS.
b. Cell abundance based on estimates from LRS.
c. estimates are based on the lowest values from references.
d. Hawkings *et al.*, 2014.
e. Measurements made May 9 - October 14.
f. Fettweis, 2007.
g. Dittmar and Kattner, 2003.
h. Lawson *et al.*, 2014b.
i. Wadham *et al.*, submitted, particulate N based on 2015 Leverett outflow data (0.12 μg mL^{-1}; Kohler, Zarsky, Stibal *et al.*, unpublished), and mean sediment loads from LRS (1.088 g L^{-1}; Hawkings *et al.*, 2014).
j. Hawkings *et al.*, 2016.
k. Estimated from mean Lena river (Cauwet and Sidorov, 1996) and Mackenzie River (Emmerton et al., 2008) DOP concentrations, and discharge volumes (Dittmar and Kattner, 2003).
l. Sorokin and Sorokin, 1996, Garneau *et al.*, 2006.
m. Percentage based on TOP.
n. Percentage based on DOP.

downstream fjord, estuary and delta environments. Our estimates of cell export from the GrIS were calculated using mean freshwater runoff values and prokaryotic abundance estimates from four glacial outlets in southwest Greenland. These estimates neither account for cell loss or freshwater flux from solid ice discharge or tundra runoff, which together amount to approximately two thirds of the freshwater flux from Greenland (Bamber *et al.*, 2012), nor do they consider the transportation of eukaryotes from the glacial environment. Supraglacial communities have been found to vary spatially across the GrIS (Cameron *et al.*, 2016), and we therefore envisage that subglacial GrIS communities will similarly vary spatially as a result of changing environmental conditions such as bedrock geology and nutrient availability, as has been considered in subglacial systems previously (Stibal *et al.*, 2012a). We therefore consider that our estimates of cells release are conservative and oversimplified, however they nonetheless provide a valuable first insight into the potential biological significance of the GrIS to downstream environments.

In summary, bacteria and archaea were exported from Leverett Glacier, an outlet of the Greenland Ice Sheet, in the order of 8.30 x 10^4 cells mL^{-1}, with Proteobacteria, Bacteroidetes and Actinobacteria dominating these microbial assemblages. We propose that the subglacial environment is the primary source of biomatter that passes LRS and KRS sample sites. Since biomass release scales with discharge, we hypothesise that as meltwater from the GrIS increases in a warming world, so too will the displacement of subglacial biota to surrounding ecosystems. The role that these microbes play in estuaries is at present poorly described, therefore investigation into how these communities are assembled is timely during this current period of deglaciation.

Experimental procedures

Study sites

The Watson River overrides Archaen gneiss and granite (Henriksen *et al.*, 2009) and is made up of two main tributaries that drain four major lobes of the GrIS in southwestern Greenland, including, from north to south, Russell, Leverett, Ørkendalen and Isorlersuup glaciers (Fig. 1). Leverett Glacier has a hydrologically active drainage area of ~600 km^2 (Cowton *et al.*, 2012). Russell and Leverett glacial melt rivers combine to

ID: prabhakaran.m Time: 21:17 I Path: //10.18.11.53/Home$/prabhakaran.m$/JW-EMI#160358

J_ID: EMI Customer A_ID: EMI13483 Cadmus Art: EMI13483 Ed. Ref. No.: 13483 Date: 10-August-16 Stage: Page: 8

form the Akuliarusiarsuup Kuua, which flows through the Sandflugtsdalen valley and serves as the northern tribury to the Watson River, which discharges into the Søndre Strømfjord. The southern tributary, Qinnguata Kuussua, flows through the Ørkendalen valley and drains the Ørkendalen and Isorlersuup glaciers (Lindbäck *et al*., 2014) before converging with the Akuliarusiarsuup Kuua upstream of Kangerlussuaq. The Qinnguata Kuussua is broader than the Akuliarusiarsuup Kuua, and several proglacial lakes are present. Due to difficulty in accessing the Qinnguata Kuussua it was not possible to monitor this tributary.

Sampling and measurements were undertaken between 10 May and 26 September 2012 (Supporting Information Table S1), encompassing the record breaking melt year (Tedesco *et al*., 2013). Two sampling sites were selected in order to distinguish between material immediately exiting the GrIS and upon entering the fjord. The inland Leverett River site (LRS; 67° 3.92'N, 50° 9.91'W) captured the subglacial outflow waters from Leverett Glacier. Due to anomalously high waters making LRS inaccessible, an alternative site (LRSc; 67° 4.25'N, 50° 17.17'W) ca 5 km downstream at the confluence of Leverett and Russell glacial outflow rivers was used from 16 August onwards (three sampling events, Supporting Information Table S1; Fig. 1). The abbreviation LRS is used to refer to both sites, unless otherwise stated herein. The downstream Kangerlussuaq river site (KRS; 67° 0.30'N, 50° 41.18'W) was situated ca 27 km downstream along the Akuliarusiarsuup Kuua, below the convergence with the Qinnguata Kuusua, and immediately before the Watson River empties into the delta at the head of the Søndre Strømfjord (Fig. 1).

Discharge, sediment load and chemistry

The methods used for measuring and calculating discharge and sediment load at KRS are described in Hasholt *et al*. (2012). Discharge and sediment load were collected from 2007 until 2013. Chemical analyses of the sampled waters have been reported previously (Hawkings *et al*., 2014; 2015; 2016; Wadham *et al*., submitted) and are summarized with permission in Supporting Information Tables S2, S3 and S4. Mean particulate organic P was calculated from 6 LRS samples taken on day of year 2012 (DOY) 131, 145, 168, 177, 184 and 207 (Hawkings *et al*., 2016). Data for dissolved organic carbon (DOC) were determined by high temperature combustion catalytic oxidation (680°C) using a Shimadzu TOC-V analyser (Kyoto, Japan) with a high sensitivity catalyst, as described by Lawson *et al*. (2014b). Precision and accuracy were $< \pm$ 7% and the limit of detection was $<$1 μM.

Microbiology

For microbiological analyses, triplicate river water samples were collected into sterile 50 mL syringes and were immediately filtered through Sterivex-GP 0.22 μm polyethersulfone filters (Millipore, Billerica, MA) until the filter clogged (35 - 175 mL depending on the suspended sediment content; volumes filtered per date and location are shown in Supporting Information Table S1). Liquid was expelled from the filters, filter inlets and outlets were closed using sterile caps, and filter units were stored at −20°C within 20 minutes from collection, or were stored next to frozen icepacks for up to two hours prior to storage at −20°C. Samples were transported frozen to home laboratories in Copenhagen.

DNA extraction from filtered samples was performed no later than two weeks after collection. The filters were thawed at room temperature in a sterile laminar flow cabinet and DNA was extracted using the PowerWater Sterivex DNA Isolation Kit (MO BIO Laboratories, Carlsbad, CA) following the manufacturer's protocol. An unused Sterivex filter was extracted alongside each batch of extractions as a procedural control. These procedural controls were processed for sequence library preparation until the point of quantification.

Prokaryotic 16S rRNA genes from river sample DNA extracts were quantified, relative to the DNA extracts of artificial river water standards, by using a qPCR set-up with primer pairs 341F (5′-CCTACGGGAGGCAGCAG-3′) and 518R (5′-ATTACCGCGGCTGCTGG-3′; Muyzer *et al*., 1993) to target prokaryotic 16S rRNA genes, and 931F (5′-AGGAATTGGCGGGGGAGCA-3′; Jackson *et al*., 2001) and 1100R (5′-BGGGTCTCGCTCGTTRCC-3′; Einen *et al*., 2008) to target archaeal 16S rRNA genes. Cell abundance data was generated using qPCR analyses in combination with the mean 16S rRNA gene copy number per cell for each sample, based on reference Greengenes OTU 16S rRNA gene copy numbers per cell (Langille *et al*., 2013). The mean 16S rRNA gene copy number per cell of the standard inoculant mix was 2.18 ± 0.40 copies cell-1 for prokaryotes and 3.00 ± 0.00 copies cell-1 for archaea. The mean 16S rRNA gene copy number per cell of the samples was 2.98 ± 0.23 copies cell-1 for prokaryotes and 1.83 ± 0.47 copies cell-1 for archaea based on non-rarefied amplicon diversity. Reaction mixtures (20 μL total) consisted of 1 μL of template DNA, 10 μL of SYBR Premix DimerEraser (TaKaRa, Japan) and 0.8 μL of the forward and reverse primers (10 pmol μL^{-1}). The cycle program was 95°C for 30 s followed by 50 cycles of 95°C for 30 s, 55°C for 30 s for primer pair 341F-518R, or 64°C for 30 s for primer pair 931F-1100R, and 72°C for 30 s. The reaction was completed by a final 72°C elongation step for 6 min and followed by high-resolution melt curve analysis in 0.5°C increments from 55 to 98°C. The abundance of bacteria and archaea in the samples was determined using qPCR on a CFX96 Touch real-time PCR detection system (Bio-Rad, CA). All qPCR reactions were performed in duplicate and were prepared under DNA free conditions in a pressurized clean-lab with a HEPA filtered air inlet and nightly UV-irradiation. Beyond the filtration of samples through Sterivex-GP 0.22 μm polyethersulfone filters, no further steps were taken to prevent or quantify the amplification of extracellular DNA. In order to achieve accurate cell abundance quantification unbiased by DNA extraction, procedural qPCR standards were prepared. Heat-sterilised (450°C for 8 hours) river sediment from the Watson River delta was re-suspended in autoclaved deionised water using a ratio of 2 g sediment per litre in order to simulate the natural river sediment load. Cultures of the aerobic heterotroph *Variovorax paradoxus* (Betaproteobacteria), methanotroph *Methylosinus sporium* (Alphaproteobacteria) and methanogen *Methanosphaerula palustris* (Euryarchaeota), representing typical components of a subglacial community (Stibal *et al*., 2012), were counted using epifluorescence microscopy and then immediately added to the

ID: prabhakaran.m Time: 21:17 I Path: //10.18.11.53/Home$/prabhakaran.m$/JW-EMI#160358

sediment suspension in a 9:1:1 ratio to obtain a final concentration of 1.1 x 10^9 cells g^{-1} sediment. Serial dilutions (1:10) of the artificial river water were prepared to generate five further concentrations, down to 1.1 x 10^4 cells g^{-1} sediment. A blank standard containing no cells was also included. Each procedural standard (60 mL) was filtered through a Sterivex filter. Filters were then sealed with sterile caps and frozen at −20°C for at least 24 h, before DNA was extracted from them following the same protocol as for the samples.

Sequence library preparation from DNA extracts, sequencing and downstream quality filtering and analysis was performed as described in Cameron *et al.*, 2016, with the exception that samples were rarefied to 8670 sequences per sample. This protocol has been included as supplementary information. All negative and procedural controls that were processed for sequence library preparation had a final DNA concentration of $\leq$0.8 ng mL^{-1}, therefore these amplicons were not sequenced. Operational taxonomic units (OTU) were defined as sequences that possessed $\geq$ 97% identity. Amplicon data are available at The European Bioinformatics Institute under study accession number PRJEB12394. (http://www.ebi.ac.uk).

Statistical analyses

CatchAll (Bunge, 2011) was used to calculate parametric alpha diversity. Untransformed Bray–Curtis resemblance and analysis of similarity (ANOSIM) were calculated from OTU matrices using PRIMER-E version 6 (Plymouth, UK). Multivariate statistical analysis was used to explain the variation in the community composition data as a function of sample location and environmental variables. The relative abundance data were arcsin$\sqrt{x}$ transformed prior to analysis. All data were standardised and centred. Detrended canonical correspondence analysis (DCCA) was used to determine the length of the gradient along the first ordination axis in order to select the appropriate method for ordination of the data. A combination of unconstrained and constrained analysis was used to explain the variation in the data. Interactive forward selection with 999 Monte Carlo permutations was used in the constrained analysis. The *p* values were corrected for multiple testing using false discovery rate. All multivariate data analyses were performed using the software Canoco 5 (Microcomputer Power, NY).

Acknowledgements

This research was funded by Danish Research Council grants FNU 10-085274 to CJ and CENPERM DNRF100. It has additionally been supported by a NERC grant NE/I008845/1 to JLW, and by a Czech Science Foundation grant GACR 15-17346Y to MS. We thank Pernille Stockmarr for technical assistance.

References

Adams, H.E., Crump, B.C., and Kling, G.W. (2014) Metacommunity dynamics of bacteria in an arctic lake: the impact of species sorting and mass effects on bacterial production and biogeography. *Front Microbiol* **5:**82.

Bamber, J., Van Den Broeke, M., Ettema, J., Lenaerts, J., and Rignot, E. (2012) Recent large increases in freshwater fluxes from Greenland into the North Atlantic. *Geophys Res Lett* **39:** L19501.

Bartholomew, I., Nienow, P., Sole, A., Mair, D., Cowton, T., Palmer, S., and Wadham, J. (2011) Supraglacial forcing of subglacial drainage in the ablation zone of the Greenland ice sheet. *Geophys Res Lett* **38:** L08502.

Bhatia, M.P., Kujawinski, E.B., Das, S.B., Breier, C.F., Henderson, P.B., and Charette, M.A. (2013) Greenland meltwater as a significant and potentially bioavailable source of iron to the ocean. *Nat Geosci* **6:** 274–278.

Bunge, J. (2011) Estimating the number of species with CatchAll. *Biocomputing* 121–130.

Cameron, K.A., Hagedorn, B., Dieser, M., Christner, B.C., Choquette, K., Sletten, R., *et al.* (2015) Diversity and potential sources of microbiota associated with snow on western portions of the Greenland Ice Sheet. *Environ Microbiol* **17:** 594–609.

Cameron, K.A., Stibal, M., Zarsky, J.D., Gözdereliler, E., Schostag, M., and Jacobsen, C.S. (2016) Supraglacial bacterial community structures vary across the Greenland ice sheet. *FEMS Microbiol Ecol* **92:** fiv164.

Cauwet, G., and Sidorov, I. (1996) The biogeochemistry of Lena River: organic carbon and nutrients distribution. *Mar Chem* **53:** 211–227.

Chandler, D.M., Wadham, J.L., Lis, G.P., Cowton, T., Sole, A., Bartholomew, I., *et al.* (2013) Evolution of the subglacial drainage system beneath the Greenland Ice Sheet revealed by tracers. *Nat Geosci* **6:** 195–198.

Clason, C.C., Mair, D.W.F., Nienow, P.W., Bartholomew, I.D., Sole, A., Palmer, S., and Schwanghart, W. (2015) Modelling the transfer of supraglacial meltwater to the bed of Leverett Glacier, southwest Greenland. *Cryosphere* **8:** 123–138.

Comiso, J.C. (2006) Arctic warming signals from satellite observations. *Weather* **61:** 70–76.

Cowton, T., Nienow, P., Bartholomew, I., Sole, A., and Mair, D. (2012) Rapid erosion beneath the Greenland ice sheet. *Geology* **40:** 343–346.

Crump, B.C., Adams, H.E., Hobbie, J.E., and Kling, G.W. (2007) Biogeography of bacterioplankton in lakes and streams of an arctic tundra catchment. *Ecology* **88:** 365–1378.

Crump, B.C., Amaral-Zettler, L.A., and Kling, G.W. (2012) Microbial diversity in arctic freshwaters is structured by inoculation of microbes from Soils. *ISME J* **6:** 1629–1639.

Dieser, M., Broemsen, E.L.J.E., Cameron, K.A., King, G.M., Achberger, A., Choquette, K., *et al.* (2014) Molecular and biogeochemical evidence for methane cycling beneath the western margin of the Greenland Ice Sheet. *isme J* **8:** 2305–2316.

Dittmar, T. and Kattner, G. (2003) The biogeochemistry of the river and shelf ecosystem of the Arctic Ocean: a review. *Mar Chem* **83:** 103–120.

Einen, J., Thorseth, I.H., and Øvreås, L. (2008) Enumeration of archaea and bacteria in seafloor basalt using real-time quantitative PCR and fluorescence microscopy. *FEMS Microbiol Lett* **282:** 182–187.

Emmerton, C.A., Lesack, L.F.W., and Vincent, W.F. (2008) Nutrient and organic matter patterns across the Mackenzie River, estuary and shelf during the seasonal recession of sea-ice. *J Marine Syst* **74:** 741–755.

Fagerbakke, K.M., Heldal, M., and Norland, S. (1996) Content of carbon, nitrogen, oxygen, sulfur and phosphorus in native aquatic and cultured bacteria. *Aquat Microb Ecol* **10:** 15–27.

Fettweis, X. (2007) Reconstruction of the 1979–2006 Greenland ice sheet surface mass balance using the regional climate model MAR. *Cryosphere Discussions* **1:** 123–168.

Fettweis, X., Tedesco, M., Van Den Broeke, M., and Ettema, J. (2011) Melting trends over the Greenland ice sheet (1958–2009) from spaceborne microwave data and regional climate models. *Cryosphere* **5:** 359–375.

Fettweis, X., Franco, B., Tedesco, M., Van Angelen, J.H., Lenaerts, J.T.M., Van Den Broeke, M.R., and Gallée, H. (2012) Estimating Greenland ice sheet surface mass balance contribution to future sea level rise using the regional atmospheric climate model MAR. *Cryosphere* **7:** 3101–3147.

Fukuda, R., Ogawa, H., Nagata, T., and Koike, I. (1998) Direct determination of carbon and nitrogen contents of natural bacterial assemblages in marine environments. *Appl Environ Microbiol* **64:** 3352–3358.

Garneau, M.-., Vicent, W.F., Alonso-Sáez, L., Gratton, Y., and Lovejoy, C. (2006) Prokaryotic community structure and heterotrophic production in a river-influenced coastal Arctic ecosystem. *Aquat Microb Ecol* **42:** 27–40.

Gutiérrez, M.H., Galand, P.E., Moffat, C., and Pantoja, S. (2015) Melting glacier impacts community structure of Bacteria, Archaea, and Fungi in a Chilean Patagonia fjord. *Environ Microbiol* **17:** 3882–3897.

Hallet, B., Hunter, L., and Bogen, J. (1996) Rates of erosion and sediment evacuation by glaciers: A review of field data and their implications. *Glob Planet Change* **12:** 213–235.

Hamilton, T.L., Peters, J.W., Skidmore, M.L., and Boyd, E.S. (2013) Molecular evidence for an active endogenous microbiome beneath glacial Ice. *isme J* **7:** 1402–1412.

Hanna, E., Huybrechts, P., Steffen, K., Cappelen, J., Huff, R., Shuman, C., *et al.* (2008) Increased runoff from melt from the Greenland Ice Sheet: A response to global warming. *J Climate* **21:** 331–341.

Hasholt, B., Bobrovitskaya, N., Bogen, J., Mcnamara, J., Mernild, S.H., Milburn, D., and Walling, D.E. (2006) Sediment transport to the Arctic Ocean and adjoining cold oceans. *Hydrol Res* **37:** 413–432.

Hasholt, B., Mikkelsen, A.B., Nielsen, M.H., and Larsen, M.A.D. (2012) Observations of runoff and sediment and dissolved loads from the Greenland ice sheet at Kangerlussuaq, West Greenland, 2007 to 2010. *Z Geomorphol* **57:** 3–27.

Hawkings, J.R., Wadham, J.L., Tranter, M., Raiswell, R., Benning, L.G., Statham, P.J., *et al.* (2014) Ice sheets as a significant source of highly reactive nanoparticulate iron to the oceans. *Nat Commun* **5:** 3929.

Hawkings, J.R., Wadham, J., Tranter, M., Lawson, E., Sole, A., Cowton, T., *et al.* (2015) The effect of warming climate on nutrient and solute export from the Greenland Ice Sheet. *Geochem Perspect Lett* **1:** 94–104.

Hawkings, J., Wadham, J., Tranter, M., Telling, J., Bagshaw, E., Beaton, A., *et al.* (2016) The Greenland Ice Sheet as a hotspot of phosphorus weathering and export in the Arctic. *Glob Biogeochem Cy* **30:** 191–210.

Henriksen, N., Higgins, A.K., Kalsbeek, F., Pulvertaft, T., and Christopher, R. (2009) Greenland from Archaean to Quaternary: descriptive text to the 1995 Geological map of Greenland, 1: 2 500 000. Geological Survey of Denmark and Greenland Bulletin 18.

Holmes, R.M., Peterson, B.J., Gordeev, V.V., Zhulidov, A.V., Meybeck, M., Lammers, R.B., and Vörösmarty, C.J. (2000) Flux of nutrients from Russian rivers to the Arctic Ocean: Can we establish a baseline against which to judge future changes? *Water Resour Res* **36:** 2309–2320.

Hudson, B., Overeem, I., McGrath, D., Syvitski, J.P.M., Mikkelsen, A., and Hasholt, B. (2014) MODIS observed increase in duration and spatial extent of sediment plumes in Greenland fjords. *Cryosphere* **8:** 1161–1176.

Irvine-Fynn, T.D.L., Edwards, A., Newton, S., Langford, H., Rassner, S.M., Telling, J., *et al.* (2012) Microbial cell budgets of an Arctic glacier surface quantified using flow cytometry. *Environ Microbiol* **14:** 2998–3012.

Jackson, C.R., Langner, H.W., Donahoe, -Christiansen, J., and Inskeep, W.P McDermott, T.R. (2001) Molecular analysis of microbial community structure in an arsenite-oxidizing acidic thermal spring. *Environ Microbiol* **3:** 532–542.

Kim, J.H., Kim, J.H., Wang, P., Park, B.S., and Han, M.S. (2016) An improved quantitative real-time PCR assay for the enumeration of *Heterosigma akashiwo* (Raphidophyceae) cysts using a DNA debris removal method and a cyst-based standard curve. *PLoS ONE* **11:** e0145712.

Langille, M.G.I., Zaneveld, J., Caporaso, J.G., McDonald, D., Knights, D., Reyes, J.A., *et al.* (2013) Predictive functional profiling of microbial communities using 16S rRNA marker gene sequences. *Nat Biotech* **31:** 814–821.

Lawson, E.C., Bhatia, M.P., Wadham, J.L., and Kujawinski, E.B. (2014a) Continuous summer export of nitrogen-rich organic matter from the Greenland Ice Sheet inferred by ultrahigh resolution mass spectrometry. *Environ Sci Technol* **48:** 14248–14257.

Lawson, E.C., Wadham, J.L., Tranter, M., Stibal, M., Lis, G.P., Butler, C.E.H., *et al.* (2014b) Greenland Ice Sheet exports labile organic carbon to the Arctic oceans. *Biogeosciences* **11:** 4015–4028.

Leeson, A.A., Shepherd, A., Briggs, K., Howat, I., Fettweis, X., Morlighem, M., and Rignot, E. (2014) Supraglacial lakes on the Greenland ice sheet advance inland under warming climate. *Nat Clim Chang* **5:** 51–55.

Liang, Z., and Keeley, A. (2013) Filtration recovery of extracellular DNA from environmental water samples. *Environ Sci Technol* **47:** 9324–9331.

Lindbäck, K., Pettersson, R., Doyle, S.H., Helanow, C., Jansson, P., Kristensen, S.S., *et al.* (2014) High-resolution ice thickness and bed topography of a land-terminating section of the Greenland Ice Sheet. *Earth Syst Sci Data* **6:** 331–338.

Mernild, S.H., Liston, G.E., Hiemstra, C.A., and Christensen, J.H. (2010) Greenland ice sheet surface mass-balance modeling in a 131-yr perspective, 1950-2080. *J Hydrometeorol* **11:** 3–25.

Mindl, B., Anesio, A.M., Meirer, K., Hodson, A.J., Laybourn-Parry, J., Sommaruga, R., and Sattler, B. (2007) Factors influencing bacterial dynamics along a transect from supraglacial runoff to proglacial lakes of a high Arctic glacieri. *FEMS Microbiol Ecol* **59:** 307–317.

Montross, S.N., Skidmore, M., Tranter, M., Kivimäki, A.-L., and Parkes, R.J. (2013) A microbial driver of chemical weathering in glaciated systems. *Geology* **41:** 215–218.

Muyzer, G., De Waal, E.C., and Uitterlinden, A.G. (1993) Profiling of complex microbial populations by denaturing gradient gel electrophoresis analysis of polymerase chain reaction-amplified genes coding for 16S rRNA. *Appl Environ Microbiol* **59:** 695–700.

Nielsen, K.M., Johnsen, P.J., Bensasson, D., and Daffonchio, D. (2007) Release and persistence of extracellular DNA in the environment. *Environ Biosafety Res* **6:** 37–53.

Rignot, E., Velicogna, I., Van Den Broeke, M.R., Monaghan, A., and Lenaerts, J.T.M. (2011) Acceleration of the contribution of the Greenland and Antarctic ice sheets to sea level rise. *Geophys Res Lett* **38:** L05503.

Savio, D., Sinclair, L., Ijaz, U.Z., Parajka, J., Reischer, G.H., Stadler, P., *et al.* (2015) Bacterial diversity along a 2600 km river continuum. *Environ Microbiol* **17:** 4994–5007.

Sharp, M., Parkes, J., Cragg, B., Fairchild, I.J., Lamb, H., and Tranter, M. (1999) Widespread bacterial populations at glacier beds and their relationship to rock weathering and carbon cycling. *Geology* **27:** 107–110.

Shepherd, A., Ivins, E.R., A., G., Barletta, M.J. Bentley, M.J., Bettadpur, S., *et al.* (2012) A reconciled estimate of ice-sheet mass balance. *Science* **338:** 1183–1189.

Skidmore, M.L., Foght, J.M., and Sharp, M.J. (2000) Microbial life beneath a High Arctic glacier. *Appl Environ Microbiol* **66:** 3214–3220.

Sorokin, Y.I. and Sorokin, P.Y. (1996) Plankton and primary production in the Lena River estuary and in the south-eastern Laptev Sea. *Estuarine Coastal Shelf Sci* **43:** 399–418.

Stibal, M., Hasan, F., Wadham, J.L., Sharp, M.J., and Anesio, A.M. (2012a) Prokaryotic diversity in sediments beneath two polar glaciers with contrasting organic carbon substrates. *Extremophiles* **16:** 255–265.

Stibal, M., Wadham, J.L., Lis, G.P., Telling, J., Pancost, R.D., Dubnick, A., *et al.* (2012b) Methanogenic potential of Arctic and Antarctic subglacial environments with contrasting organic carbon sources. *Glob Chang Biol* **18:** 3332–3345.

Stibal, M., Gözdereliler, E., Cameron, K.A., Box, J.B., Stevens, I.T., Gokul, J.K., *et al.* (2015a) Microbial abundance in surface ice on the Greenland Ice Sheet. *Front Microbiol* **6:** 225.

Stibal, M., Schostag, M., Cameron, K.A., Hansen, L.H., Chandler, D.M., Wadham, J.L., and Jacobsen, C.S. (2015b) Different bulk and active bacterial communities in cryoconite from the margin and interior of the Greenland ice sheet. *Environ Microbiol Rep* **7:** 293–300.

Tedesco, M. (2007) A new record in 2007 for melting in Greenland. *Eos, Trans Am Geophys Union* **88:** 383–383.

Tedesco, M., Fettweis, X., Mote, T., Wahr, J., Alexander, P., Box, J.E., and Wouters, B. (2013) Evidence and analysis of 2012 Greenland records from spaceborne observations, a regional climate model and reanalysis data. *Cryosphere* **7:** 615–630.

Tranter, M., Skidmore, M., and Wadham, J. (2005) Hydrological controls on microbial communities in subglacial environments. *Hydrol Process* **19:** 995–998.

Wadham, J.L., Tranter, M., Skidmore, M., Hodson, A.J., Priscu, J., Lyons, W.B., *et al.* (2010) Biogeochemical weathering under ice: Size matters. *Glob Biogeochem Cy* **24:** GB3025.

Wadham, J.L., De'ath, R., Monteiro, F.M., Tranter, M., Ridgwell, A., Raiswell, R., and Tulaczyk, S. (2013) The potential role of the Antarctic Ice Sheet in global biogeochemical cycles. *Earth Env Sci T R So* **104:** 1–13.

Wilhelm, L., Besemer, K., Fasching, C., Urich, T., Singer, G.A., Quince, C., and Battin, T.J. (2014) Rare but active taxa contribute to community dynamics of benthic biofilms in glacier-fed streams. *Environ Microbiol* **16:** 2514–2524.

Yde, J.C., Finster, K.W., Raiswell, R., Steffensen, J.P., Heinemeier, J., Olsen, J., *et al.* (2010) Basal ice microbiology at the margin of the Greenland ice sheet. *Ann Glaciol* **51:** 71–79.

Supporting information

Additional supporting information may be found in the online version of this article at the publisher's web-site.

Table S1. Sampling dates (day of year 2012) and water volumes (ml) filtered through Sterivex filters at each site. [a]; LRS sample date, [b]; KRS sample date, [c]; outburst event (Hawkings *et al.*, 2014), d; Leverett and Russell glacial outflow river confluence (LRSc).

Table S2. Nutrient concentrations of sampled waters (μM). b.d. - below detection. CNFe; colloidal/nanoparticulate Fe. References are depicted with superscript letters; [a] Wadham *et al.*, submitted, [b] Hawkings *et al.*, 2016, [c] Hawkings *et al.*, 2014, [d] Hawkings *et al.*, in review.

Table S3. Major ion concentrations of sampled waters ($\mu eq\ l^{-1}$) from Hawkings *et al.*, 2015.

Table S4. Particulate P analyses (μM) from Hawkings *et al.*, 2016.